# LAPS v1.0.0: Lagrangian Advection of Particles at Sea, a Matlab program to simulate the displacement of particles in the ocean.

Maxime Mouyen[1], Romain Plateaux[2], Alexander Kunz[3], Philippe Steer[4], and Laurent Longuevergne[4]

[1]Department of Earth Space and Environment, Chalmers University of Technology SE-412 96 Gothenburg, Sweden
[2]YouWol Asia-Pacific, Taipei, Taiwan
[3]Department of Geosciences, National Taiwan University, Taipei, Taiwan
[4]Univ Rennes, CNRS, Geosciences Rennes - UMR 6118, F-35000 Rennes, France

**Correspondence:** Maxime Mouyen (maxime.mouyen@chalmers.se)

**Abstract.** We develop a Matlab program named LAPS (Lagrangian Advection of Particles at Sea) to simulate the advection of suspended particles in the global ocean with a minimal user effort to install, set and run the simulations. LAPS uses the 3D sea current velocity fields provided by ECCO2 to track the fate of suspended particles injected in the ocean, at specific places and times, during a period of time. LAPS runs with a short configuration file set by the user and returns the distribution of the particles at the end of the advection. A continuous tracking option is also available to record the complete trajectory of the particles throughout the entire period of advection. The effect of water waves, or Stokes drift, which alter sea surface current velocities, can also be taken into account. The principle and usage of the program is detailed and then applied to three case studies. The first two cases studies are applied to suspended sediment transport. We show how LAPS simulations can be used to investigate the spatio-temporal distribution of fine particles observed by satellites in the upper ocean. We also estimated sediment deposit areas on the seafloor as a function of sediment grain sizes. The third case study simulates the dispersion of microplastic particles during a tropical cyclone, and shows how the Stokes drift, which is significant during storm events, alters the particles trajectories compared to the case where the Stokes drift is neglected.

## 1 Introduction

The quantitative analysis of particle transport by ocean currents relies on in-situ and remote observations, and on Lagrangian simulation of particle transport (van Sebille et al., 2018). The latter allows hypothesis testing and statistical analysis when observations are missing. Indeed, remote sensing observations are global and are focused on sea surface. By contrast, in-situ ocean observations, from ships or drifters, can probe deeper water but remain local. Thus, Lagrangian simulation allows to bridge the gap between different spatial scales of observations.

For instance, sediments eroded from the continent are advected until they finally settle in deep oceanic basins. The finest particles remain in suspension for a long time, making wide structures that are visible by remote sensing satellites (Martinez et al., 2015). Then for greater depths, the Lagrangian simulation of particle transport allows evaluating where they eventually accumulate and build sediment deposits (Mouyen et al., 2018). The ocean also spreads living organisms over the globe and Lagrangian simulation can explain how biological dissemination toward the most remote areas is possible (Fraser et al.,

2017, 2018). Ocean transport is also at the core of the contemporary issue of plastic littering, forming large accumulations of
25   plastic debris in the northern Pacific gyre (Egger et al., 2020) and elsewhere. Once again, Lagrangian simulation of particle
transport allows to study these contemporary issues within a global framework (Lebreton et al., 2012).

   Several Lagrangian simulation software exist, with various computation and customization ability (van Sebille et al., 2018).
Here we present such a Lagrangian simulation program, named LAPS (Lagrangian Advection of Particles at Sea) and pro-
grammed with Matlab. LAPS simulates the Lagrangian transport of the particles under the effect of oceanic currents and, if
30   requested, waves action (Stokes drift). The oceanic currents are computed by the Estimating the Circulation and Climate of
the Ocean 2 (ECCO2) consortium (Menemenlis et al., 2008). The Stokes drift velocities are provided by the Ifremer and are a
reanalysis of the WAVEWATCH III model (Rascle and Ardhuin, 2013). Although no novel numerical method is used compared
to already existing Lagrangian simulation software, we believe LAPS offers new interesting features. LAPS is very simple to
use since it requires no installation and no programming, but only an input file defining the position of the particles to be
35   transported and a short configuration file that will set about ten basic parameters, such as the time of simulation. In addition,
the program puts an emphasis on particles transport at depth, first because ECCO2 provides 3D velocity fields but also because
particles can be set to sink (e.g. due to their mass) with respect to the bathymetry used in ECCO2.

   In this article, we will first describe the method and the complete procedure to use LAPS. We then show three case studies
applied to sediment transport and movement of microplastic particles in the ocean. They shall emphasize the main simulation
40   features of this program.

## 2   Method

### 2.1   Overview

LAPS simulates the advection of particles at sea under the influence of global oceanic circulation, gravity and Stokes drift.
The velocities of the current come from ECCO2 (Menemenlis et al., 2008) for the global oceanic circulation and a reanalysis
45   of the WAVEWATCH III model for the Stokes drift (Rascle and Ardhuin, 2013). These two datasets must be downloaded by
the user before running LAPS, or at least ECCO2 if the Stokes drift is not relevant for the purpose of the simulation (below a
few meters depth for instance, as we described in a next section.) The main principle of the program is thus to attribute each
particle a velocity according to their location in the velocity grids. The initial position of each particle is provided as an input
file by the user. The position of each particle is updated every 15 minutes (simulation time) during the entire simulation period,
50   according to the current velocity at the location of the particle. The injection of particle in the ocean can be done either once,
at the beginning of the simulation, or every day until a given date.

   The ECCO2 velocity fields used in LAPS have a time resolution of 3 days and a spatial resolution of $0.25°$. Dealing with such
a large grid size can represent a computational challenge for Lagrangian models. Therefore, LAPS is designed to efficiently
manage the ECCO2 grid by only uploading the spatial and temporal data of interest. When the simulation goes beyond three
55   days, it loads a new ECC02 field and continues the advection. To work with smaller velocity field matrices and decrease the
computation time, the program loads only a sub-region of the global ECCO2 velocity field. This sub-region fits the extreme

position of the particles, with a margin of 6 geographical degrees, in order to handle the displacement of the particle over the three simulation days during which the file will be used. The same approach is used with the Stokes drift data, except that they are updated every 3 simulation-hours.

60     The simulation stops when the end date set by the user is reached, or when all particles are either set on the seafloor or beached on the coast. The two latter conditions are tested at every advection step and aim at stopping the simulation as soon as no particle can move, which may occur before the actual end of simulation. All the particles beached or settles on the seafloor are progressively removed from the advection process, to lower the computation time. Note that the program does not support parallel computing. The best way to benefit from parallel computing facilities is to split the particle input file into several input

65     files that shall be run simultaneously. LAPS does not provide functions to implement this approach, which must be designed by users willing to do so. At the end of simulation, LAPS stores the final positions of particles and, optionally their trajectories, in folders defined by the user in the configuration file. The date of the simulation and a few particle properties, mostly defining how they can sink, are also defined in the configuration, which in total requires 13 simple inputs from the user.

## 2.2   Oceanic currents

70     The oceanic currents used in LAPS are the 3-dimensions velocity fields obtained from ECCO2 (Estimating the Circulation and Climate of the Ocean 2). These products assimilate data such as sea surface height from Topex/Poseidon, Jason-1 and Jason-2 missions and ocean bottom pressure from the Gravity Recovery and Climate Experiment (GRACE (Tapley et al., 2004)) mission into a global circulation model (MITgcm (Marshall et al., 1997)) through a Green functions approach that allows to efficiently adjust the model parameters, initial conditions, and boundary conditions (Menemenlis et al., 2005b, a). They are

75     available for the 1992-present time period at a time resolution of three days and a spatial resolution of 0.25 degree. This velocity field is provided for up to 50 levels of water depths, ranging in thickness from 10 m near the surface to approximately 450 m at a maximum model depth of 6150 m from the sea surface down to the sea floor.

## 2.3   Wave action - Stokes drift

Sea surface waves can drag particles in the direction of the wave propagation. This process, also known as the Stokes drift, has
80     a significant impact on particle advection at sea, especially during storms (Fraser et al., 2018; Dobler et al., 2019). Stokes drift velocities derived from wave hindcasts based on the WAVEWATCH III® model (WW3, Tolman, 2009) and forced by winds (Rascle and Ardhuin, 2013) provided by Ifremer at a three-hours sampling can be added to the ECCO2 velocities. Adding the Stokes drift velocity provides a more accurate sea surface velocity field, and can be especially relevant to account for storm events on the particle transport (Fig. 1).

85     The spatial resolution of the Stokes drift velocity fields is 0.5 degree and its time resolution is 3 hours. LAPS provides a function that converts these velocity fields to the same spatial resolution as ECCO2, prior to any advection simulation. Thus, it is only necessary to locate the particles in the ECCO2 field, then its latitude and longitude indices can be re-used for the Stokes drift velocity field. This saves computation time because locating the particles is computationally demanding.
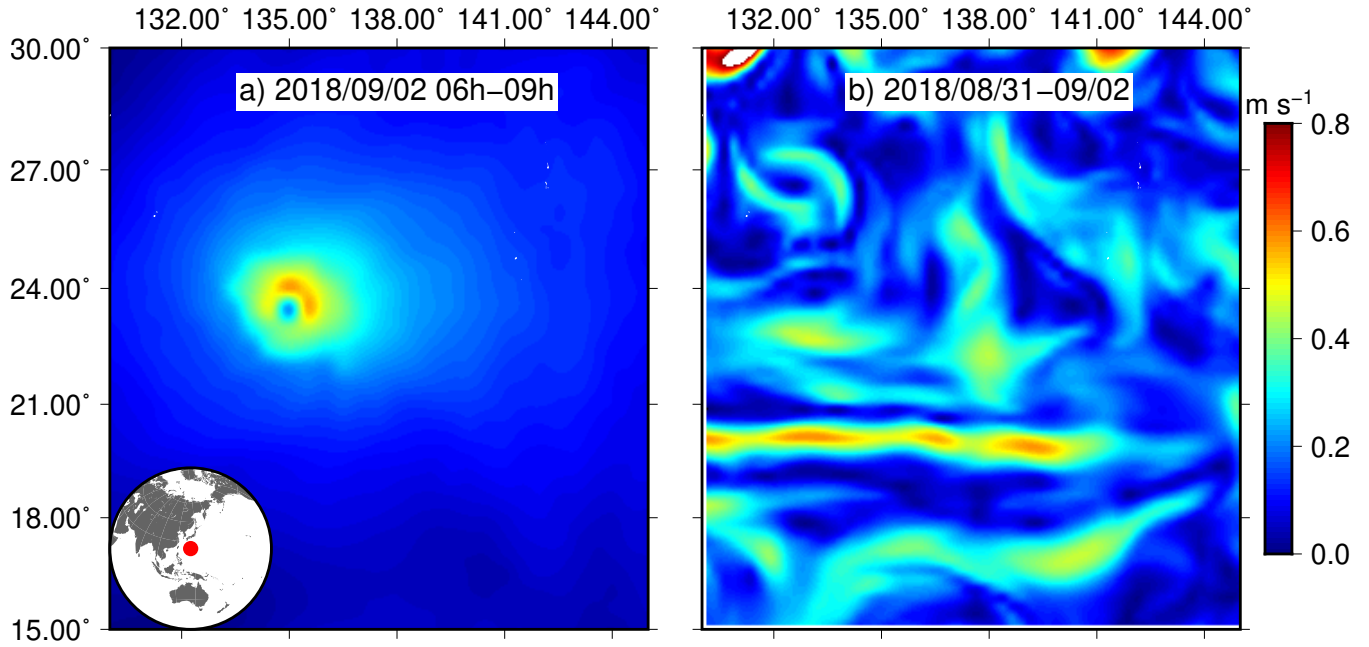
**Figure 1.** a) Stokes drift velocity in the Philippine Sea while tropical storm Jebi is traveling toward East Asia. The rather circular area of higher Stokes drift velocity is due to the higher winds of the storm. The WW3 frame is on 2018-09-02, between 6 AM and 9 AM UTC. b) Sea surface velocity at the equivalent time period, i.e from 2018-08-31 to 2018-09-02, since the time step of the ECCO2 files is 3 days.

The Stokes drift velocity is maximal at the sea surface and rapidly decreases with depth. LAPS approximates the effect of
the depth on the Stokes drift velocity, which is given in Equation 1 (Lynch et al., 2015, eq. 10.52)

$$U_w(z) = U_{w0} - \frac{U_*}{\kappa} \ln \left| \frac{z}{z_0} \right| \tag{1}$$

where $U_w(z)$ and $U_{w0}$ are the Stokes drift velocities at depth $z$ and at the sea surface, respectively, $U_*$ is the frictional velocity,
$\kappa$ is the von Karman constant and $z_0$ is the roughness length ($0.5\,\mathrm{mm} \leq z_0 \leq 1.5\,\mathrm{mm}$). With the typical approximations
$U_{w0} = 0.03W_{10}$ and $U_* = 0.0012W_{10}$ (Lynch et al., 2015), where $W_{10}$ is the wind velocity 10 m above the sea level, $U_w(z)$
can be simplified as Equation 2

$$U_w(z) = U_{w0} \left( 1 - \frac{0.04}{\kappa} \ln \left| \frac{z}{z_0} \right| \right) \tag{2}$$

Thus, we can approximate the Stokes drift velocity at depth $z$ from its surface value, the von Karman constant and the roughness length, which are set by default to $\kappa = 0.4$ and $z_0 = 1\,\mathrm{mm}$, respectively. Fig. 2 shows the rapid decrease of $U_w(z)/U_{w0}$
i.e. the term in brackets in Equation 2, as the depth increases, for three different values of $z_0$. For $z_0 = 1\,\mathrm{mm}$, the default value
set in LAPS, the Stokes drift velocity at 10 m depth decreases by a factor 10 compared to its value at the sea surface, and by a
factor 100 at 25 m depth, consistent with the fact that the Stokes drift mainly impact particles located in shallow waters. This
is especially relevant for buoyant particles such as micro-plastic debris and very fine sediment particles ($1\,\mu\mathrm{m}$) that sink at a
slow rate.

Thus, when the Stokes drift is taken into account, LAPS sets the particle velocity $U_p(z)$ following Equation 3:

$$U_p(z) = U_{ECCO2}(z) + U_{w0}c(z) \qquad (3)$$

where $U_{ECCO2}(z)$ is the depth-dependent velocity of ECCO2 and $c(z)$ is the factor that account for the decrease of the Stokes drift surface velocity (Fig. 2 and Equation 2), using $\kappa = 0.4$ and $z_0 = 1$ mm.
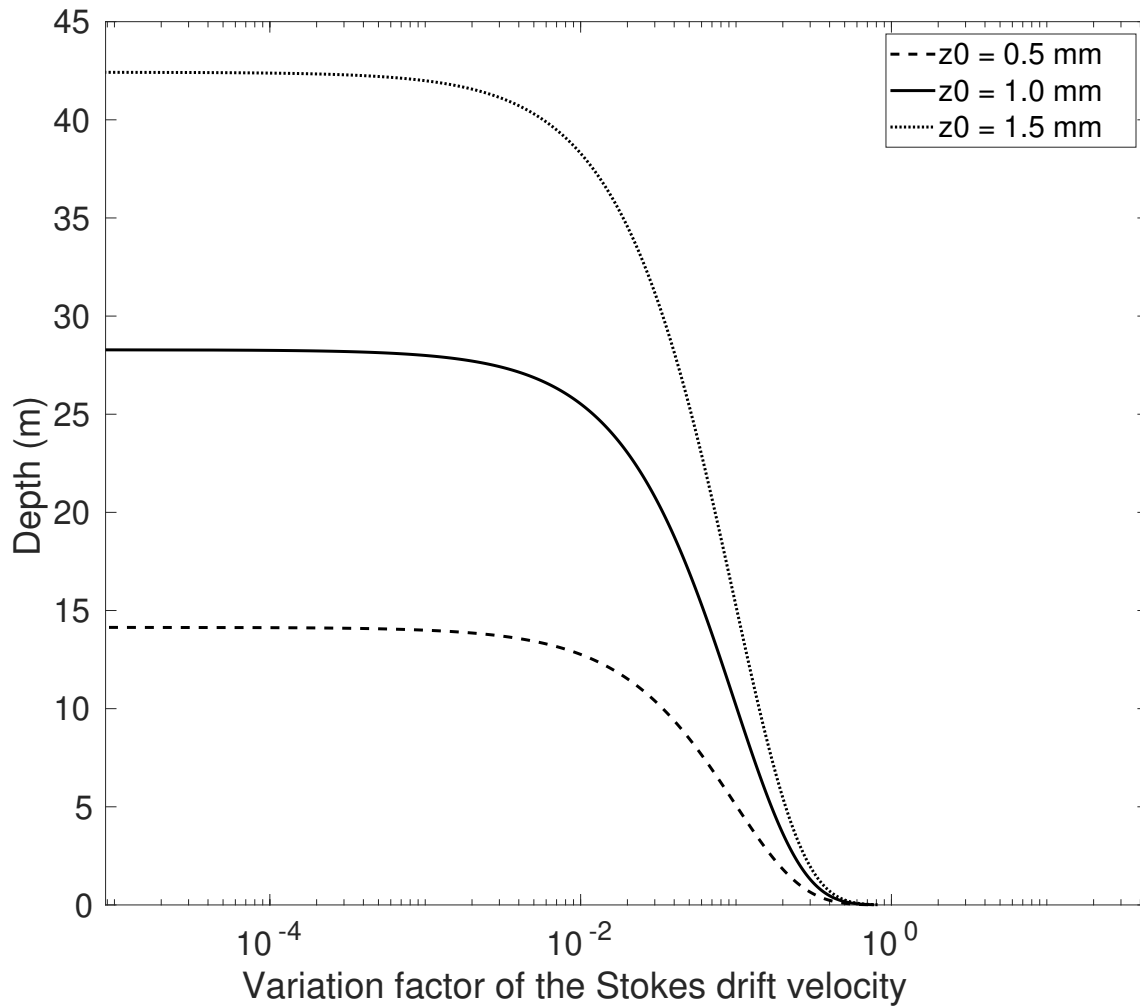
**Figure 2.** Effect of increasing depth on the evolution of Stokes drift velocity for the boundary and mean values of the roughness length $z_0$.

## 2.4 Settling of particles

Non-buoyant suspended particles, such as sediment particles, will sink at the Stokes settling velocity, expressed in Equation 4

$$v_s = D^2 g \frac{\rho_p - \rho_s}{18\mu} \qquad (4)$$

**Table 1.** Examples of times needed by particles of increasing sizes to settle on an average abyssal plain at 5000 m depth, assuming no vertical currents. The particle density is $\rho_p = 2000 \ \mathrm{kg \ m^{-3}}$.

| Particle size ($\mu$m) | Time to settle at 5000 m depth |
| --- | --- |
| 1 | 420 years |
| 5 | 17 years |
| 10 | 4 years |
| 30 | 6 months |
| 50 | 2 months |
| 70 | 1 month |
| 100 | 15 days |

where $g$ is the mean gravitational acceleration, $\rho_s = 1030 \ \mathrm{kg \ m^{-3}}$ and $\mu = 1.4 \ 10^{-3} \ \mathrm{Pa \ s}$ are the seawater density and dynamic viscosity, respectively. This formalism presupposes that the sinking particles are spherical with $\rho_p$ and $D$ the particle density and diameter, respectively, which are set by the user. The settling velocity is added to the vertical component of the oceanic currents and is the main factor governing how long a particle can remain in suspension at sea (Table 1).

115    Microplastic particles are assumed as fully buoyant at the beginning of each advection simulation. Nevertheless, they can start sinking with a given probability after they spend a certain amount of time at sea, about a few tens of days, as a result of degradation and biofouling (Fazey and Ryan, 2016; Liubartseva et al., 2018). Both this age threshold and the probability of sinking have default values that can be modified by the user. The microplastic particles that are old enough to sink are then chosen randomly with respect to that probability. The sinking velocity of these particles is set to 0.016 m s$^{-1}$ by default

120    following the study of Kaiser et al. (2017) and can also be changed by the user. The diversity of biofouling processes, plastic types and local parameters at sea do not allow a definitive estimation of such values. That is why it is defined as a user parameter that can be easily modified to any other estimated value.

## 3    Workflow and algorithm

### 3.1    Workflow

125    The main task for the user is to write a configuration file that sets up the simulation parameters (an example of such configuration file is provided with the program). Aside from paths and the simulation dates, the user must only specify another 5 or 6 parameters:

1. if the Stokes drift should be enabled

2. if the particles should be tracked at regular time intervals, as opposed to only the final positions

130    3. if the particles are micro-plastic debris or suspended sediment, which control the settling of the particles (see section 2.4). Sediment particles will sink at the Stokes settling velocity, which requires to specify the diameter and density of the sediment particle. Choosing micro-plastic debris means that particles either stay at the surface or may sink after a user-defined time at sea, with also user-defined probability and velocity.

See the online documentation and the example configuration file for setting such parameters.

135    The user should then download the ECCO2 velocity for the zonal (ECCO2, 2021a), meridional (ECCO2, 2021b) and vertical (ECCO2, 2021c) components fields and the WW3 Stokes drift provided by the Ifremer institute that are suitable for the simulation time-period (e.g. for 2016: Ifremer, 2016).

When running the simulation, the program checks if the parameters of the configuration file are correct and if the needed velocity fields exist. If any check fails, explicit error messages will be displayed in the Matlab's command window, so the user

140    can fix them. If all checks pass, the simulation starts.

The progress is indicated by printing the processed injection time in the command window. The time of computation depends mostly on the simulation period and the amount of particles that must be advected. The tracking option can also significantly increase the computation time, because it updates a matrix storing each particle position at the time interval requested by the user. See runtime examples for different settings in Table 2. At the end of the simulation, the results are saved in the folder

145    defined by the user in the configuration file.

**Table 2.** Examples of runtime for different simulation settings. The Stokes drift is always enabled. CPU is Intel(R) Xeon(R) E5-2630 v3 @ 2.40GHz.

| Np | $t_S$ | Injection | Tracking | Runtime |
|----|-------|-----------|----------|---------|
| 10 | 1 year | first day | every 1 hour | 2 min |
| 10 | 1 year | every day | no tracking | 2 min |
| 10 | 1 year | every day | every 1 hour | 2 hours |
| 100 | 1 year | first day | no tracking | 2 min |
| 100 | 1 year | every day | no tracking | 4 min |
| 100 | 1 year | first day | every 1 hour | 15 min |
| 1000 | 1 year | first day | no tracking | 2.5 min |
| 1000 | 1 year | first day | every 1 hour | 2.6 hours |

## 3.2    Algorithm

A simplified algorithm is presented in Algorithm 1. It takes ECCO2 or a combination of ECCO2 and Stokes drift (see section 2.3) as well as particles initial positions as inputs. The main while-loop runs until the final time of simulation set by the user is reached. It performs the injection of particles and updates the particle position for each time step of 15 mins, according to

150 current velocity where the particle is located. The latter step thus implies to locate each particle in the current 3-D velocity field, which is done using the Matlab function `histc`.

---

**Algorithm 1** Algorithm advection. $T$ is the current time in the simulation, $TF$ is the final time of simulation, $TSI$ is the final time of particle injection. $dT$ is the time increment of the simulation (15 min).

---

**Require:** Configuration file, ECCO2 3-D velocity field and initial locations of the particles

**Require:** (optional) Stokes drift (SD) 3-D velocity field

**Ensure:** Valid configuration file

**Ensure:** ECCO2 and SD files match the simulation time period3

  **while** $T < TF$ AND particles can still move **do**

    **if** $T < TSI$ AND $T =$ new day **then**

      Inject particles at the initial location

    **end if**

    Find particles velocities $V$ in the 3-D velocity field

    Update particles positions $X = X + V.dT$

    Update time $T = T + dT$

    Count particles that can still move

  **end while**

  **return** Particles positions at the end of the simulation

  **return** (optional) Particles trajectories

---

The validity of the simulation relies on the fact that each particle is properly located in the 3-D velocity field and that it moves according to that local current velocity at its position. In addition, since the velocity field changes at regular time interval, the program must track the simulation time and load a new velocity field whenever the end of such a time interval is reached. We

155 validate that these constraints are respected by creating synthetic ECCO2 and Stokes drift velocity fields, with simple velocity components: 1 m s$^{-1}$ in pure east, west south and north directions split on four equal longitudinal sections. One particle is set in each of this section and the simulation is run over 5 days of transport, a time long enough to necessitate loading a new velocity field (ECCO2 has a 3-days resolution). We ensured that the simulated particles trajectories and distances agree with the expected results. The synthetic velocity fields, the simulation results and their analysis are archived together with the program

160 LAPS.

## 4 Comparison with surface drifters

We evaluate the general performance of LAPS by comparing its simulation results with surface drifter data acquired in the frame of the Global Drifter Program (GDP, Elipot et al., 2016a), specifically the global hourly location from GDP surface drifters tracked by GPS (Elipot et al., 2016b). We select drogued drifters that are available between years 2015 and 2019 (2837

165 drifters in total), extract their positions at the earliest time and run LAPS for particles injected at those same initial time and

positions. The simulation is done over one year, tracking the simulated positions every 6 hours. This leads to a maximum of $365 \times 24/6 = 1460$ positions per drifter. The drogue, or sea anchor, is centered around 15 m depth and attach to the float with tether. A drogued drifter will thus drift with the velocity of the currents at 15 m depth. For that reason, the particles in the simulation are injected at 15 m depth. The Stokes drift is not accounted for because it is likely negligible at such depth, about

170 10 times smaller than at the surface according to Fig. 2. Fig. 3 shows two examples of such a comparison between simulated and observed drifters trajectories
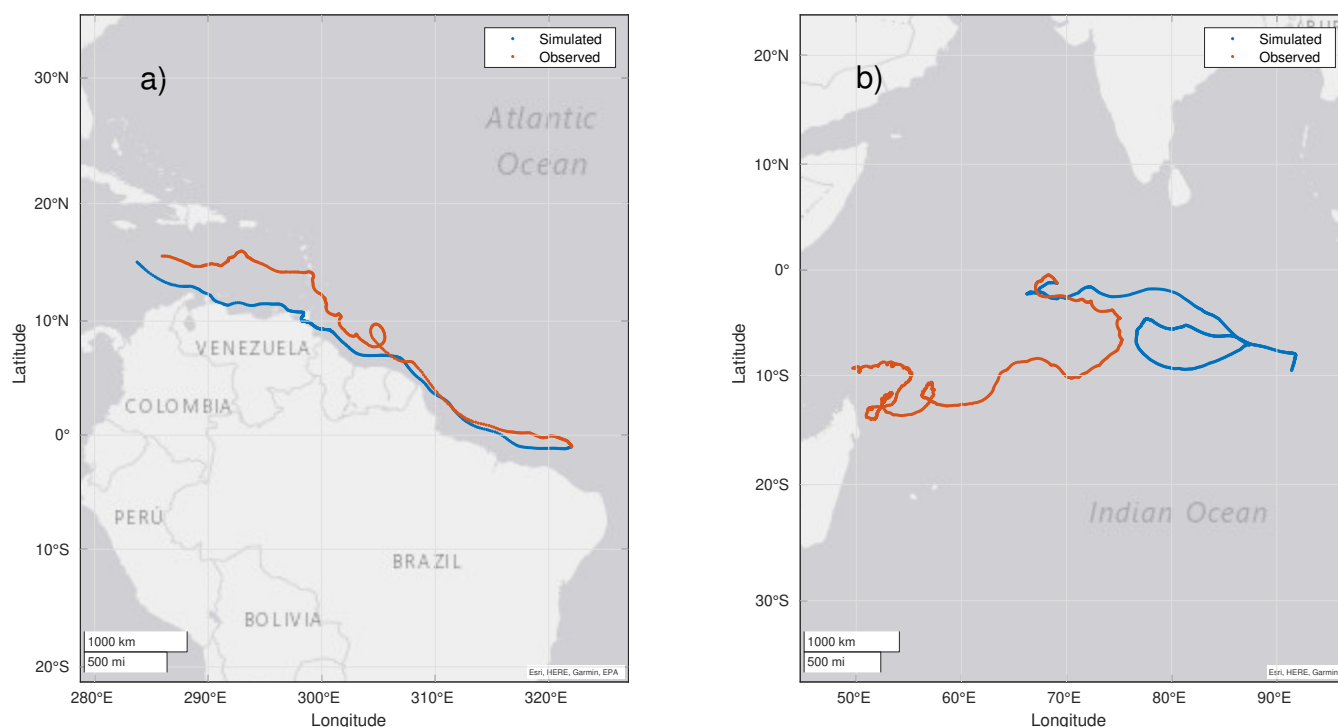
**Figure 3.** Comparisons between simulated and observed drifters trajectories for two end-members examples showing a) satisfactory and b) unsatisfactory LAPS trajectory predictions.

To quantify the uncertainty of LAPS, we compare the observed and simulated position vectors for each 6-hourly observed and simulated positions, for all drifters during the entire year of simulation. The origin of each position vector is the initial position of each drifter (the simulated and observed initial positions are identical). Residual vectors are then computed by

175 subtracting each pair of positions vector. Fig. 4 a shows the 2-D (East-North) distribution of the residuals, with their histograms along the North and East axis in Figs. 4 b and c, respectively.
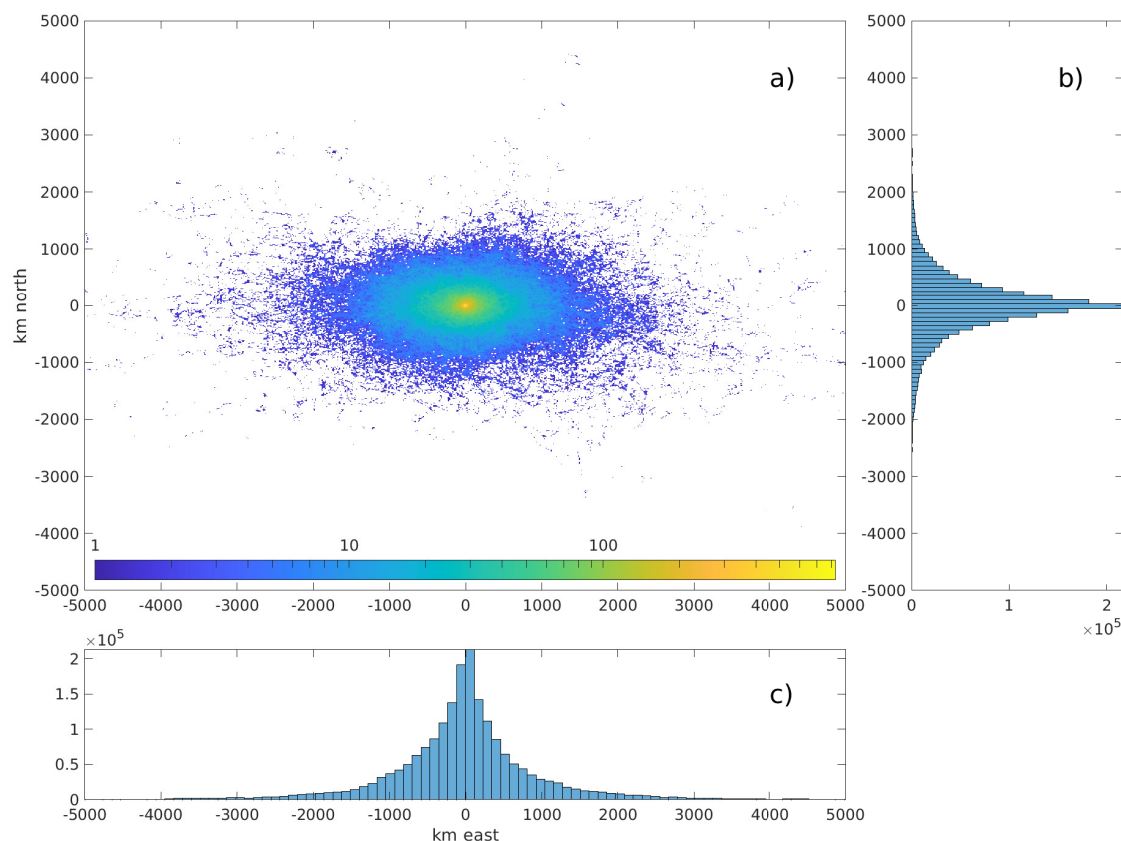
**Figure 4.** Residuals between the observed and simulated drifter positions for trajectories computed over one year and tracked every 6 hours. a) Distribution of the amplitude of the residuals in the East and North component. b) Histogram of the residuals for the North component. c) Histogram of the residuals for the East component.

One limitation in this comparison is that, because of its size (about 40 cm diameter) the buoy of the drifter, even drogued, is much more sensitive to winds than a particle floating just at the surface or below. Nevertheless, this comparison helps to provide an uncertainty of the particle positions. The standard deviation of the residuals is 1060 km for the East component and 560 km for the North component. Given the area covered by the global ocean, we consider that the standard deviations obtained with LAPS are reasonable.

## 5   Case studies and discussion

In this section, we show and discuss the results of two examples of application of LAPS. The first example focuses on the spatio-temporal distribution of suspended material discharged by the Amazon River in 2019. The second one simulates movement of

185   microplastic particles in the ocean, with an emphasis on the effect of Stokes drift on the particle trajectories in an area hit by a tropical cyclone.

### 5.1   Spatiotemporal distribution of suspended material in the ocean

About 19 Gt yr$^{-1}$ of suspended sediment are discharged by rivers into the oceans (Milliman and Farnsworth, 2011) and take part in various processes, such as building delta fans or fuelling the nutrient cycle that sustains marine life (Darby et al., 2016).

190   Therefore, simulating the oceanic transport of sediment discharged by rivers can provide useful constraints on the spatio-temporal distribution of sediment, which is difficult to assess in-situ due to the wide areas and depths ranges of the ocean.

In this section, we compare the spatio-temporal distribution of fine particles (1 $\mu$m diameter) simulated by LAPS to that of the gelbstoff and detritus observed by the MODIS (Moderate Resolution Imaging Spectroradiometer) Aqua satellite mission (NASA Goddard Space Flight Center et al., 2018).

195   For the LAPS simulation, 345 particle inputs are evenly distributed every 0.25° along the Brazilian coast, within a ribbon of 30 km width running from latitudes 5° south up to 10° north, in Guyana, which includes the Amazon estuary. One particle is released from each of the input at a constant rate, every day since 2015 until the end of 2019. Note that the rate of sediment input might not be strictly constant through time, especially for the Amazon where a seasonal sediment delivery is reported (Martinez et al., 2009). We neglect this time variation because we are only interested in the first order patterns of the simulations.

200   The simulations outputs are saved only in 2019, every month for days 1, 5, 10, 20, 25 and 28. One monthly spatial distribution of the particles is the average of these seven days. We then compute the relative difference between each monthly spatial distribution and the monthly average over the entire year, and convert it into a percentage. The resulting distributions are shown in the left column of Fig. 5. We compute equivalent monthly maps using MODIS-Aqua data, using the monthly and yearly composite products available online(NASA Goddard Space Flight Center et al., 2018) for year 2019 using the 9 km-resolution

205   (Fig. 5, right column).
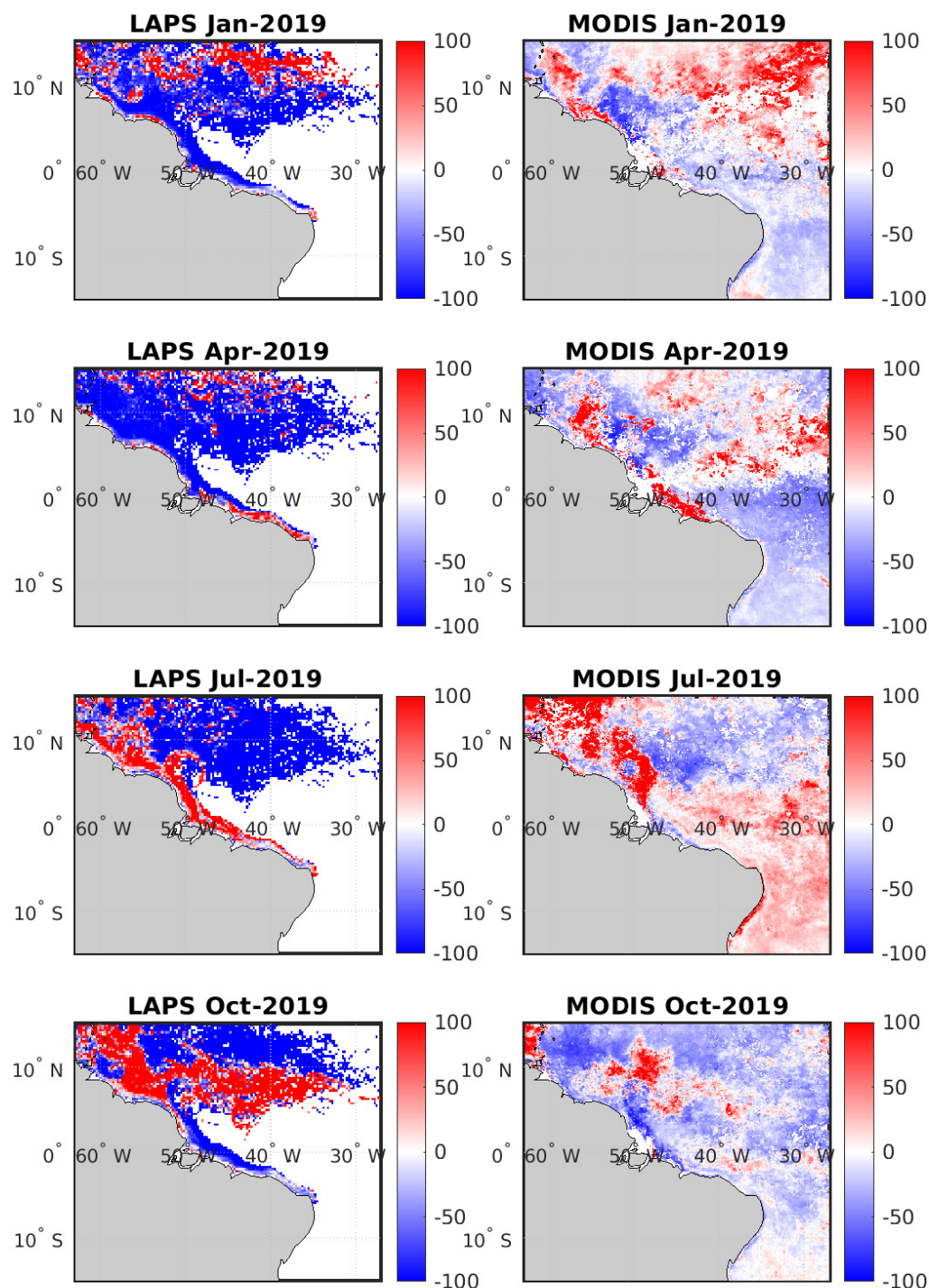
**Figure 5.** Relative spatial distribution of fine sediment particles at the sea surface (0 to 1 m depth) simulated by LAPS (left column) and observed by MODIS satellite (right column), every three months in 2019.

The simulation cannot account for all the processes and the variety of material that compose the gelbstof. In addition, the actual particles input leading to MODIS-Aqua observations covers larger areas and time periods than the one we simulated in LAPS. Rather we intend to compare the spatiotemporal pattern of slowly sinking particles out of the basin with one of the world largest sediment discharge (1.43 Gt yr$^{-1}$, (Milliman and Farnsworth, 2011)). Indeed, we observe common features:

210    1. Particles are transported eastward in January and April, and north-westward In July and October

2. South of the Amazon estuary, we note a relative increase of particle content in April and relative decrease in October.

Conversely, LAPS can also be used to highlight inconsistencies between observations and simulations in order to better identify sediment sources and grain size. In addition, optical observations are restricted to the sea surface and the transport of sediment that sank deeper shall take advantage from such simulations. LAPS can thus be used to investigate sediment transport

215    for various grain size distributions. Indeed, as already shown in Table 1, sediment grain sizes control their settling velocity and, therefore, significantly alter how sediment distribute in the water column.

## 5.2    Deposition zones of suspended sediment

Here we simulate the area of deposition of the suspended sediment delivered by the rivers Magdalena (Colombia) and Godavari (India), which have significant sediment loads of 140 and 170 Mt yr$^{-1}$, respectively. We use the "Sediment mode" of LAPS to

220    evaluate how the sediment deposition area might be controlled by the grain size of the sediment, ranging from 25 to 95 $\mu$m, with 10 $\mu$m increase. Indeed, for a given density, the size of grain is responsible for most of the variation of particle settling velocities.

The simulation runs from January 2015 to December 2019 with particles injected every day outside the river from January 2015 to December 2018. The 1-year time lag between the end of the injection and the end of the simulation is made to ensure

225    that all injected particles can settle on the seafloor by the end of the simulation. The Stokes drift is not taken into account because the finest particles (25 $\mu$m) still sink at about 1 m hr$^{-1}$, putting them quickly at depths where the Stokes drift influence has vanished.

The results in Fig. 6 show that, overall, fine grain size extend further than coarser ones, simply because they need more time to settle and can thus travel over longer distances. However, the shape of the sedimentation zone is a rather complex

230    combination of the sea-floor depth (as given in ECCO2), the grain size and the sea current velocities, from which we expect to obtain realistic estimate of contemporary sedimentation zones.

## 5.3    Ocean plastic pollution

The pollution of the marine environment with macro and microplastic debris is rising and has become a global problem (Borrelle et al., 2020). It is estimated that more than 5 trillion plastic particles weighing 250,000 tons float on the ocean

235    surface (Eriksen et al., 2014) and that in the top 200 m of the Atlantic Ocean alone up to 21.1 million tons of plastic are floating (Pabortsava and Lampitt, 2020). The global distribution of floating plastic particles is roughly understood, and the main accumulation spots in large ocean gyres are mapped (Avio et al., 2017; Cózar et al., 2014). However, it is still unclear
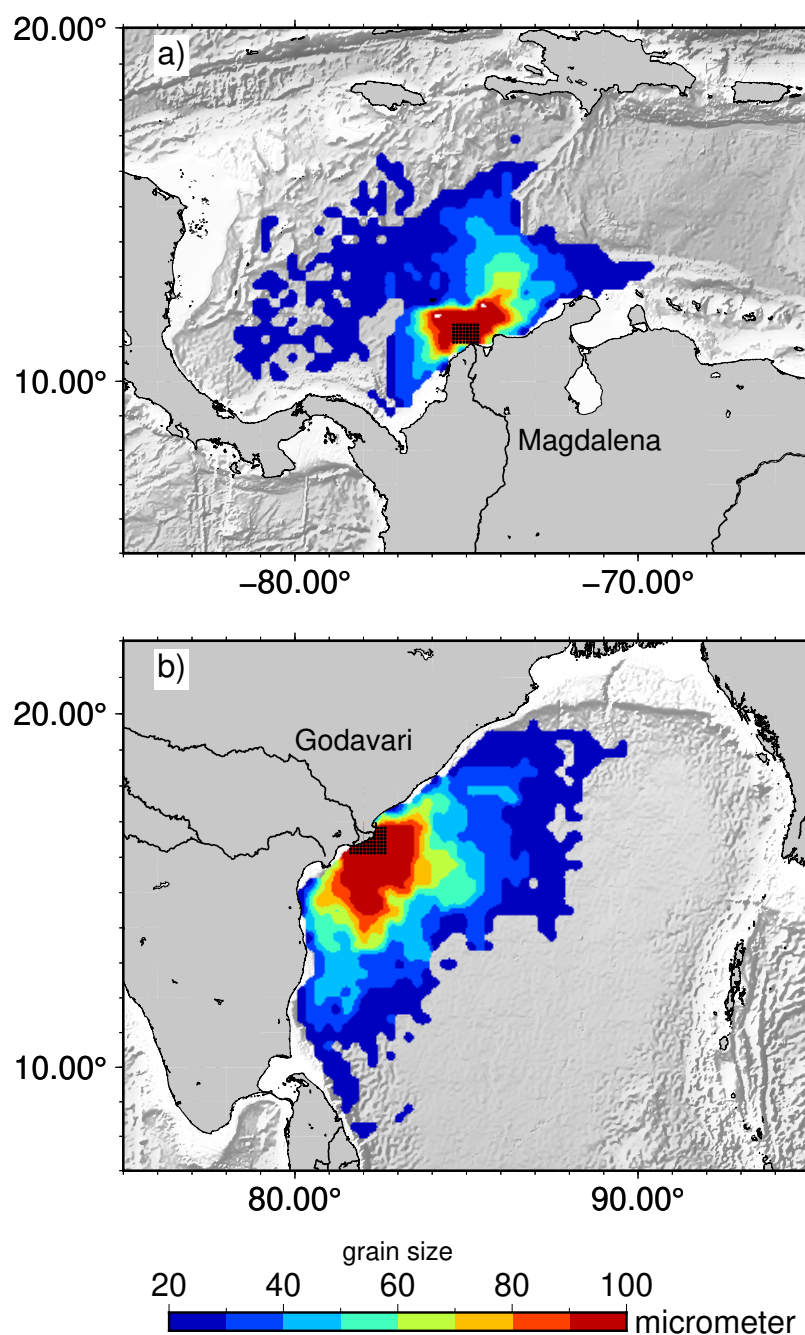
**Figure 6.** Sedimentation zones for the a) Magadalena river b) Godavari river and grain sizes ranging from 25 to 95 $\mu$m, with 10 $\mu$m increase. The shaded bathymetry is from Etopo (NOAA, 2009). The black dots at the exit of each river locate where the sediment particles are injected.

how much plastic sank to the bottom of the sea and where. Barrett et al. (2020) estimated that 14 million tons of plastic particles accumulated at the seafloor in the Great Australian Bight. Studying the pollution in the ocean or deep sea is a difficult task,
240   due to the vast areas and great depths that need to be covered (Jalón-Rojas et al., 2019; Hardesty et al., 2017; Goldstein et al., 2013). Therefore, modelling the transport and sinking of plastic particles is of great interest as it allows to estimate the location of pollution hotspots at the sea surface as well as in the deep sea. Additionally, in recent years, it has become more and more evident that rivers play a major role in polluting the oceans with plastic (Jambeck, 2015; Lebreton et al., 2017). It was estimated that every year 1.15-2.41 million tons of plastic waste are carried by rivers into the ocean (Lebreton et al., 2017). The fate of
245   riverine plastic waste is not well known. Modelling can help to identify the transport ways and the locations where plastic might sink to the ocean floor or is beached on the coast. These results can in turn help to plan mitigation or cleaning efforts. We use LAPS to run two different scenarios, scenario 1 shows the release of plastic particles by rivers in East-Asia and in scenario 2 we demonstrate the impact of a typhoon on the particle trajectory.

### 5.3.1   Scenario 1

250   In this scenario, we use the Tamsui River in Taiwan, and the Pearl River and Yangtze River in China as examples for riverine plastic output. All three rivers carry significant amounts of micro and macroplastic waste into the ocean (Lin et al., 2018; Wong et al., 2020; Schneider et al., 2021; Zhang et al., 2021) and belong to the most polluting rivers worldwide (Jambeck et al., 2015; Lebreton et al., 2017). For this scenario, 20 injection points are randomly placed at the river mouth. The injection of particles is done once on May 1st, 2019 and the trajectories are simulated until July 30th, 2019. Three different settings for LAPS are
255   used while keeping location of starting points and time frame of the model the same:

- a) no Stokes drift affecting the particles

- b) Stokes drift affecting the particles

- c) same as (b) but with additional sinking of microplastic particles. The parameters are set so that particles at sea for more than 50 days may sink with a probability of 0.4 and a sinking velocity of 0.02 m s$^{-1}$. These parameters were
260       chosen based on the study of Karkanorachaki et al. (2021).

The resulting trajectories are shown in Fig. 7a, b and c, respectively, and it can be seen that Stokes drift has a significant influence on the particle trajectories. Especially for the particles that were released by the Pearl River. Without Stokes drift, the majority of particles traveled from the Pearl River mouth in a north-eastern direction. Some particles beached at the north coast of Taiwan, others continued further northwards. However, when applying Stokes drift in the model, all particles released
265   by the Pearl River stay in a gyre close to the river mouth. For particles that were released by the Tamsui River and the Yangtze River, the effect of Stokes drift results in different trajectories and endpoints as well. Without Stokes drift, particles from the Tamsui River end at the eastern coast of Japan, whereas with Stokes drift particles travel to the western coast of Japan. This scenario shows that Stokes drift is an important factor to consider, as it can change the result of a model and its interpretation significantly. Microplastic sinking results only in a reduced travel distance of particles. This effect is stronger

270 for longer modeling times, as the probability for sinking increases. However, parameters for microplastic sinking should be chosen with care. As summarized by Karkanorachaki et al. (2021), a variety of factors, such as plastic density, shape, particle size, biofouling, waves, are controlling the sinking of plastic particles. Currently, only basic concepts and mechanisms of microplastic sinking are known from laboratory experiments. Field studies are missing yet. Therefore, validation of the model results with real world examples are not possible.
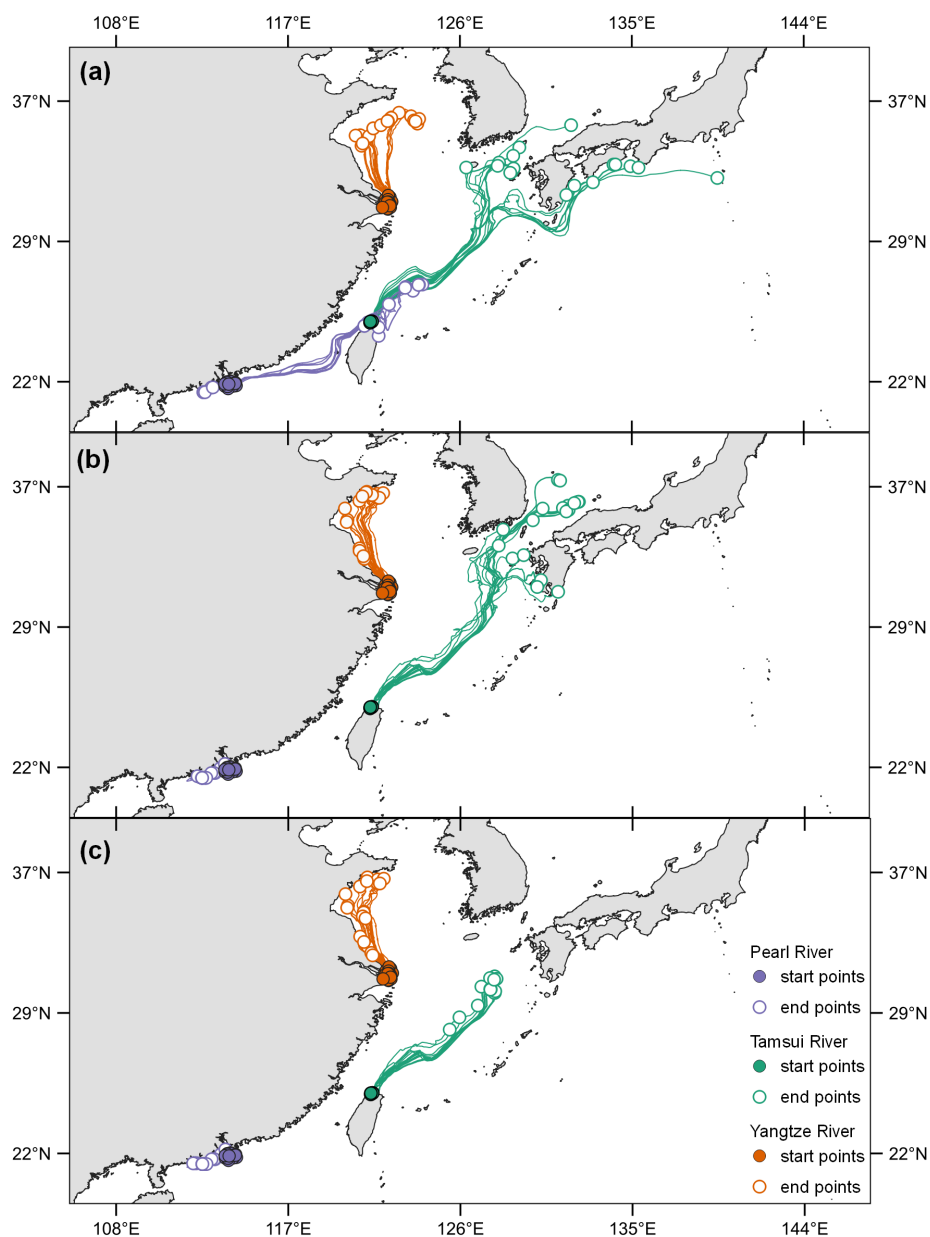
**Figure 7.** Modeling results for scenario 1. Injection of particles was on May 1st, 2019 and the model run until July 30th, 2019. The location of starting points (plain color dots) is the same for all settings. (a) Particle trajectories calculated without Stokes drift. (b) Particle trajectories calculated with Stokes drift. (c) Particle trajectories calculated with Stokes drift and sinking of microplastic particles enabled. See text for model parameters.

### 5.3.2 Scenario 2

In this scenario, the simulation is set in a period where a typhoon was passing through the area of interest. By comparing simulations with and without account for the Stokes drift, we aim at demonstrating the sensitivity of the simulation to storm events that last only a short time. Typhoon Lekima (Hanna) was a category 4 super typhoon with maximum sustained wind speed reaching up to 250 km h$^{-1}$ (Naval Meteorology and Oceanography Command, 2021). Lekima formed on July 30th 2019 and passed from August 2nd in north-western direction to the east coast of Taiwan and made landfall on August 9th in China. Ten particles were placed randomly in a small area in the eastern part of the Bashi Channel between Taiwan and the Philippines. Injection of particles was done at two different times. First injection was on May 1st 2019 and particles traveled for three months through the undisturbed western Pacific (Fig. 8a). Second injection was on July 1st 2019 and particles crossed the path of typhoon Lekima (Fig. 8b). For both time periods, the trajectories with and without Stokes drift effect were modelled.

For the time period May to July, it can be seen that Stokes drift has a significant impact on the location of the endpoints. The location of the endpoints differs in average by 1068 km, with some endpoints only 163 km apart and others up to 2422 km apart. During the time period from July to September when particles crossed the typhoon path, the trajectories are completely different from the undisturbed time period. Interestingly, the effect of Stokes drift in this case is not as strong as during the previous period. Endpoints are closer together, and locations differ in average by 625 km.
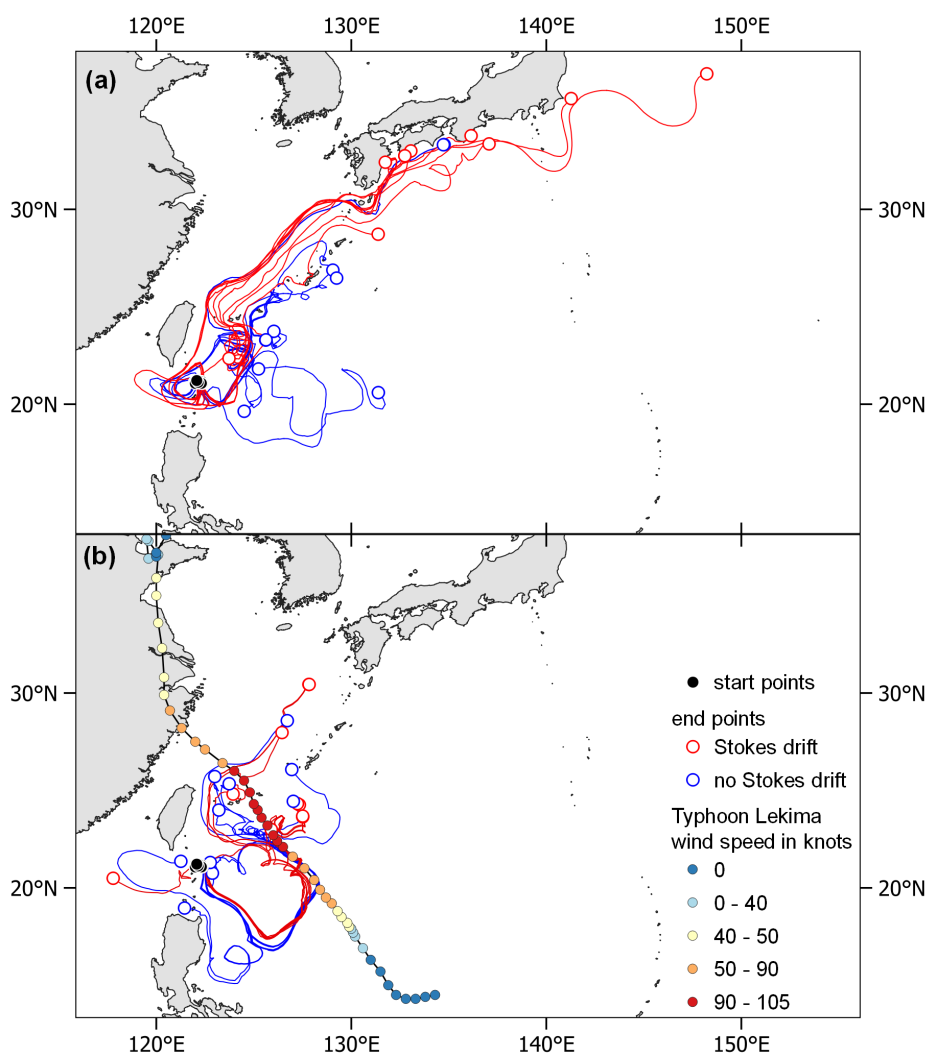
**Figure 8.** Modeling results of scenario 2. Starting location of particles was always the same. Model was run with and without Stokes drift, sinking of microplastic particles disabled. (a) Injection of particles on May 1st, 2019 and model run until July 30th, 2019. (b) Injection of particles on July 1st, 2019 and model run until September 30th, 2019. Typhoon Lekima crossed area of particle trajectories during August 5th to 8th, 2019.

## 5.4 Perspectives

Two features are considered for future development. The first one is the ability for storms and currents to re-mobilize sediment particles that settled at shallow depths (Stastna and Lamb, 2008). At the moment, a workaround is to update the particles input

file with points located in areas prone to sediment re-suspension, and to keep the injection running over the requested time. This will act as if sediment particles were re-suspended from these locations.

295  The second feature is the effect of tidal currents, which can also impact the sediment redistribution in coastal areas. The significance of this effect depends on the area considered and on the timescale at which the sediment transport is considered, since the strongest tidal currents have a 6- to 12 hours period (to be compared with the 3-days resolution of ECCO2 velocity fields used for LAPS). The last FES2014b products (Carrère et al., 2015) should be suitable for that purpose.

## 6  Conclusion

300  We described a Matlab program for Lagrangian advection that allows to simulate the 3D displacement of particles in the ocean. The utilisation of LAPS is made simple by only requesting to download publicly available current velocity data and setting a short configuration file for basic parameters (such as the time of the simulation, the paths to working directories, particle sinking or particle tracking). By comparing LAPS results with actual drifters trajectories over one year of transport, we evaluate particle position uncertainties to 1060 km for the East component and 560 km for the North component. We run

305  example of applications that show how LAPS can handle particle grain size and Stokes drift in order to simulate particles trajectories in various cases. We suggest that LAPS is suitable for investigating sediment transport, plastic littering and other suspended particles.

*Code and data availability.*  The exact version of the model used to produce the results used in this paper is archived on Zenodo (Mouyen, 2021) under the MIT licence, as are input data and scripts to run the model and produce the plots for all the simulations presented in this

310  paper (Mouyen et al., 2021).

*Video supplement.*  Two videos of the plastic advection in different situations are available on Figshare (Kunz, 2021).

*Author contributions.*  MM designed the study, designed and wrote the software, computed and analysed the results. RP helped improving the algorithm. AK run and analysed the plastic littering simulations. PS and LL helped designing the study. All authors contributed to the final manuscript.

315  *Competing interests.*  The authors declare no competing interest.

*Acknowledgements.* We thank Matthew Mazloff (UCSD-SCRIPPS) and Dimitris Menemenlis (NASA-JPL) for their insights on the addition of the Stokes drift to the ECCO2 products. AK received funding from the Ministry of Science and Technology Taiwan (R.O.C.), grant number MOST 110-2116-M-002-005-MY2. CNES and Britanny region (contract 147549) are acknowledged for financial support

# References

320    Avio, C. G., Gorbi, S., and Regoli, F.: Plastics and microplastics in the oceans: From emerging pollutants to emerged threat, Marine Environmental Research, 128, 2–11, https://doi.org/10.1016/j.marenvres.2016.05.012, 2017.

Barrett, J., Chase, Z., Zhang, J., Holl, M. M., Willis, K., Williams, A., Hardesty, B. D., and Wilcox, C.: Microplastic Pollution in Deep-Sea Sediments From the Great Australian Bight, Frontiers in Marine Science, 7, 808, https://doi.org/10.3389/fmars.2020.576170, 2020.

Borrelle, S. B., Ringma, J., Law, K. L., Monnahan, C. C., Lebreton, L., McGivern, A., Murphy, E., Jambeck, J., Leonard, G. H., Hil-
325    leary, M. A., Eriksen, M., Possingham, H. P., De Frond, H., Gerber, L. R., Polidoro, B., Tahir, A., Bernard, M., Mallos, N., Barnes, M., and Rochman, C. M.: Predicted growth in plastic waste exceeds efforts to mitigate plastic pollution, Science, 369, 1515–1518, https://doi.org/10.1126/science.aba3656, 2020.

Carrère, L., Lyard, F., Cancet, M., Guillot, A., Carrere, L., Lyard, F., Cancet, M., Guillot, A., Carrere, L., Lyard, F., Cancet, M., and Guillot, A.: FES 2014, a new tidal model on the global ocean with enhanced accuracy in shallow seas and in the Arctic region, in: European
330    Geosciences Union, edited by EGU, vol. 17 of *EGU General Assembly Conference Abstracts*, p. 5481, EGU general assembly conference abstracts, Vienna, https://doi.org/2015EGUGA..17.5481C, 2015.

Cózar, A., Echevarría, F., González-Gordillo, J. I., Irigoien, X., Úbeda, B., Hernández-León, S., Palma, A. T., Navarro, S., García-de Lomas, J., Ruiz, A., Fernández-de Puelles, M. L., and Duarte, C. M.: Plastic debris in the open ocean, Proceedings of the National Academy of Sciences of the United States of America, 111, 10 239–10 244, https://doi.org/10.1073/pnas.1314705111, 2014.

335    Darby, S. E., Hackney, C. R., Leyland, J., Kummu, M., Lauri, H., Parsons, D. R., Best, J. L., Nicholas, A. P., and Aalto, R.: Fluvial sediment supply to a mega-delta reduced by shifting tropical-cyclone activity, Nature, 539, 276–279, https://doi.org/10.1038/nature19809, 2016.

Dobler, D., Huck, T., Maes, C., Grima, N., Blanke, B., Martinez, E., and Ardhuin, F.: Large impact of Stokes drift on the fate of surface floating debris in the South Indian Basin, Marine Pollution Bulletin, 148, 202–209, https://doi.org/10.1016/j.marpolbul.2019.07.057, 2019.

ECCO2: UVEL ECCO2 cube92, https://ecco.jpl.nasa.gov/drive/files/ECCO2/cube92_latlon_quart_90S90N/UVEL.nc, 2021a.
340    ECCO2: VVEL ECCO2 cube92, https://ecco.jpl.nasa.gov/drive/files/ECCO2/cube92_latlon_quart_90S90N/VVEL.nc, 2021b.

ECCO2: WVEL ECCO2 cube92, https://ecco.jpl.nasa.gov/drive/files/ECCO2/cube92_latlon_quart_90S90N/WVEL.nc, 2021c.

Egger, M., Sulu-Gambari, F., and Lebreton, L.: First evidence of plastic fallout from the North Pacific Garbage Patch, Scientific Reports, 10, 1–10, https://doi.org/10.1038/s41598-020-64465-8, 2020.

Elipot, S., Lumpkin, R., Perez, R. C., Lilly, J. M., Early, J. J., and Sykulski, A. M.: A global surface drifter data set at hourly resolution,
345    Journal of Geophysical Research: Oceans, 121, 2937–2966, https://doi.org/10.1002/2016JC011716, 2016a.

Elipot, S., Lumpkin, R., Perez, R. C., Perez, R., Lilly, J., Early, J., and Sykulski, A.: GPS-tracked Global Hourly Drifter Data, https://www.aoml.noaa.gov/phod/gdp/hourly_data/v1.04/hourly_GPS_1.04.mat, 2016b.

Eriksen, M., Lebreton, L. C. M., Carson, H. S., Thiel, M., Moore, C. J., Borerro, J. C., Galgani, F., Ryan, P. G., and Reisser, J.: Plastic Pollution in the World's Oceans: More than 5 Trillion Plastic Pieces Weighing over 250,000 Tons Afloat at Sea, PLoS ONE, 9, 1–15,
350    https://doi.org/10.1371/journal.pone.0111913, 2014.

Fazey, F. M. and Ryan, P. G.: Biofouling on buoyant marine plastics: An experimental study into the effect of size on surface longevity, Environmental Pollution, 210, 354–360, https://doi.org/10.1016/j.envpol.2016.01.026, 2016.

Fraser, C. I., Kay, G. M., Plessis, M. d., and Ryan, P. G.: Breaking down the barrier: dispersal across the Antarctic Polar Front, Ecography, 40, 235–237, https://doi.org/10.1111/ecog.02449, 2017.

355    Fraser, C. I., Morrison, A. K., Hogg, A. M., Macaya, E. C., van Sebille, E., Ryan, P. G., Padovan, A., Jack, C., Valdivia, N., and Waters, J. M.: Antarctica's ecological isolation will be broken by storm-driven dispersal and warming, Nature Climate Change, 8, 704–708, https://doi.org/10.1038/s41558-018-0209-7, 2018.

Goldstein, M. C., Titmus, A. J., and Ford, M.: Scales of spatial heterogeneity of plastic marine debris in the northeast Pacific Ocean, PLoS ONE, 8, https://doi.org/10.1371/journal.pone.0080020, 2013.

360    Hardesty, B. D., Harari, J., Isobe, A., Lebreton, L., Maximenko, N., Potemra, J., van Sebille, E., Vethaak, A. D., and Wilcox, C.: Using Numerical Model Simulations to Improve the Understanding of Micro-plastic Distribution and Pathways in the Marine Environment, Frontiers in Marine Science, 4, 1–9, https://doi.org/10.3389/fmars.2017.00030, 2017.

Ifremer: WAVEWATCH-III HINDCAST, ftp://ftp.ifremer.fr/ifremer/ww3/HINDCAST/GLOBAL/2016_ECMWF/uss/, 2016.

Jalón-Rojas, I., Wang, X. H., and Fredj, E.: A 3D numerical model to Track Marine Plastic Debris (TrackMPD): Sensitivity of mi-
365    croplastic trajectories and fates to particle dynamical properties and physical processes, Marine Pollution Bulletin, 141, 256–272, https://doi.org/10.1016/j.marpolbul.2019.02.052, 2019.

Jambeck, J. R.: The Ocean, Climate Change 2014: Impacts, Adaptation and Vulnerability, 347, 1655–1732, https://doi.org/10.1017/CBO9781107415386.010, 2015.

Jambeck, J. R., Geyer, R., Wilcox, C., Siegler, T. R., Perryman, M., Andrady, A., Narayan, R., and Law, K. L.: Plastic waste inputs from land
370    into the ocean, Science, 347, 768–771, https://doi.org/10.1126/science.1260352, 2015.

Kaiser, D., Kowalski, N., and Waniek, J. J.: Effects of biofouling on the sinking behavior of microplastics, Environmental Research Letters, 12, 124 003, https://doi.org/10.1088/1748-9326/aa8e8b, 2017.

Karkanorachaki, K., Syranidou, E., and Kalogerakis, N.: Sinking characteristics of microplastics in the marine environment, Science of The Total Environment, 793, 148 526, https://doi.org/10.1016/j.scitotenv.2021.148526, 2021.

375    Kunz, A.: Simulations of ocean plastic littering, https://doi.org/10.6084/m9.figshare.16667302.v1, 2021.

Lebreton, L. C. M., Greer, S. D., and Borrero, J. C.: Numerical modelling of floating debris in the world's oceans, Marine Pollution Bulletin, 64, 653–661, https://doi.org/10.1016/j.marpolbul.2011.10.027, 2012.

Lebreton, L. C. M., Van Der Zwet, J., Damsteeg, J. W., Slat, B., Andrady, A., and Reisser, J.: River plastic emissions to the world's oceans, Nature Communications, 8, 1–10, https://doi.org/10.1038/ncomms15611, 2017.

380    Lin, L., Zuo, L. Z., Peng, J. P., Cai, L. Q., Fok, L., Yan, Y., Li, H. X., and Xu, X. R.: Occurrence and distribution of microplastics in an urban river: A case study in the Pearl River along Guangzhou City, China, Science of the Total Environment, 644, 375–381, https://doi.org/10.1016/j.scitotenv.2018.06.327, 2018.

Liubartseva, S., Coppini, G., Lecci, R., and Clementi, E.: Tracking plastics in the Mediterranean: 2D Lagrangian model, Marine Pollution Bulletin, 129, 151–162, https://doi.org/10.1016/j.marpolbul.2018.02.019, 2018.

385    Lynch, D. R., Greenberg, D. A., Bilgili, A., McGillicuddy Jr, D. J., Manning, J. P., and Aretxabaleta, A. L.: Particles in the coastal ocean: Theory and applications, Cambridge University Press, 2015.

Marshall, J., Adcroft, A., Hill, C., Perelman, L., and Heisey, C.: A finite-volume, incompressible Navier Stokes model for studies of the ocean on parallel computers, J. Geophys. Res., 102, 5753–5766, https://doi.org/10.1029/96JC02775, 1997.

Martinez, J. M., Guyot, J. L., Filizola, N., and Sondag, F.: Increase in suspended sediment discharge of the Amazon River assessed by
390    monitoring network and satellite data, Catena, 79, 257–264, https://doi.org/10.1016/j.catena.2009.05.011, 2009.

Martinez, J. M., Espinoza-Villar, R., Armijos, E., and Silva Moreira, L.: The optical properties of river and floodplain waters in the Amazon River Basin: Implications for satellite-based measurements of suspended particulate matter, Journal of Geophysical Research F: Earth Surface, 120, 1274–1287, https://doi.org/10.1002/2014JF003404, 2015.

Menemenlis, D., Fukumori, I., and Lee, T.: Using Green's functions to calibrate an ocean general circulation model, Monthly Weather Review, 133, 1224–1240, https://doi.org/10.1175/MWR2912.1, 2005a.

Menemenlis, D., Hill, C., Adcroft, A. J., Campin, J. M., Cheng, B., Ciotti, B., Fukumori, I., Heimbach, P., Henze, C., Kõhl, A., Lee, T., Stammer, D., Taft, J., and Zhang, J.: NASA Supercomputer Improves Prospects for Ocean Climate Research, EOS Transactions AGU, 86, 89–96, https://doi.org/10.1029/2005EO090002, 2005b.

Menemenlis, D., J-M. Campin, Heimbach, P., Hill, C., Lee, T., Nguyen, A., Schodlok, M., and Zhang, H.: ECCO2: High resolution global ocean and sea ice data synthesis, Mercator Ocean Quarterly Newsletter, 31, 13–21, http://www.mercator-ocean.fr/content/download/691/5904/version/1/file/lettre_31_en.pdf#page=13, 2008.

Milliman, J. D. and Farnsworth, K. L.: River Discharge to the Coastal Ocean: A Global Synthesis, Cambridge University Press, New York, 2011.

Mouyen, M.: LAPS, https://doi.org/10.5281/ZENODO.5187707, 2021.

Mouyen, M., Longuevergne, L., Steer, P., Crave, A., Lemoine, J. M., Save, H., and Robin, C.: Assessing modern river sediment discharge to the ocean using satellite gravimetry, Nature Communications, 9, 3384, https://doi.org/10.1038/s41467-018-05921-y, 2018.

Mouyen, M., Plateaux, R., Kunz, A., Steer, P., and Longuevergne, L.: Datasets for "LAPS v1.0.0: Lagrangian Advection of Particles at Sea, a Matlab program to simulate the displacement of particles in the ocean", https://doi.org/10.5281/ZENODO.5524113, 2021.

NASA Goddard Space Flight Center, Ocean Ecology Laboratory, and Ocean Biology Processing Group: Moderate-resolution Imaging Spectroradiometer (MODIS) Aqua Inherent Optical Properties Data; 2018 Reprocessing, doi:data/10.5067/AQUA/MODIS/L3B/IOP/2018, https://oceancolor.gsfc.nasa.gov/l3/, 2018.

Naval Meteorology and Oceanography Command: Joint Typhoon Warning Center (JTWC), https://www.metoc.navy.mil/jtwc/jtwc.html?western-pacific, 2021.

NOAA: ETOPO1 1 Arc-Minute Global Relief Model, https://www.ncei.noaa.gov/access/metadata/landing-page/bin/iso?id=gov.noaa.ngdc.mgg.dem:316, 2009.

Pabortsava, K. and Lampitt, R. S.: High concentrations of plastic hidden beneath the surface of the Atlantic Ocean, Nature Communications, 11, 1–11, https://doi.org/10.1038/s41467-020-17932-9, 2020.

Rascle, N. and Ardhuin, F.: A global wave parameter database for geophysical applications. Part 2: Model validation with improved source term parameterization, Ocean Modelling, 70, 174–188, https://doi.org/10.1016/J.OCEMOD.2012.12.001, 2013.

Schneider, F., Kunz, A., Hu, C.-S., Yen, N., and Lin, H.-T.: Rapid-survey methodology to assess litter volumes along large river systems - A case study of the Tamsui river in Taiwan, Sustainability, in press., 2021.

Stastna, M. and Lamb, K. G.: Sediment resuspension mechanisms associated with internal waves in coastal waters, Journal of Geophysical Research: Oceans, 113, https://doi.org/10.1029/2007JC004711, 2008.

Tapley, B. D., Bettadpur, S., Ries, J. C., Thompson, P. F., and Watkins, M. M.: GRACE measurements of mass variability in the Earth system, Science (New York, N.Y.), 305, 503–505, https://doi.org/10.1126/science.1099192, 2004.

Tolman, H. L.: User manual and system documentation of WAVEWATCH III TM version 3.14 †, Tech. rep., NOAA, 2009.

van Sebille, E., Griffies, S. M., Abernathey, R., Adams, T. P., Berloff, P., Biastoch, A., Blanke, B., Chassignet, E. P., Cheng, Y., Cotter, C. J., Deleersnijder, E., Döös, K., Drake, H. F., Drijfhout, S., Gary, S. F., Heemink, A. W., Kjellsson, J., Koszalka, I. M., Lange, M., Lique, C.,

MacGilchrist, G. A., Marsh, R., Mayorga Adame, C. G., McAdam, R., Nencioli, F., Paris, C. B., Piggott, M. D., Polton, J. A., Rühs, S., Shah, S. H., Thomas, M. D., Wang, J., Wolfram, P. J., Zanna, L., and Zika, J. D.: Lagrangian ocean analysis: Fundamentals and practices, https://doi.org/10.1016/j.ocemod.2017.11.008, 2018.

Wong, G., Löwemark, L., and Kunz, A.: Microplastic pollution of the Tamsui River and its tributaries in northern Taiwan: Spatial heterogeneity and correlation with precipitation, Environmental Pollution, 260, 113 935, https://doi.org/10.1016/j.envpol.2020.113935, 2020.

Zhang, Z., Deng, C., Dong, L., Liu, L., Li, H., Wu, J., and Ye, C.: Microplastic pollution in the Yangtze River Basin: Heterogeneity of abundances and characteristics in different environments, Environmental Pollution, 287, 117 580, https://doi.org/10.1016/j.envpol.2021.117580, 2021.